Number 3 Volume 13 September2006 Journal of Engineering

DYNAMIC SOIL-STRUCTURE RESPONSE ANALYSIS OF AN IRAQI SOIL BASED ON GEOPHYSICAL TESTING

Dr.Omer al-FaroukS.al-Damluji
Assistant Professor
Department of Civil Engineering
University of Baghdad,Irag

Mustafa Musa Salih
Formerly Postgraduate Student
Department of Civil Engineering
University of Baghdad,Irag

ABSTRACT

In this paper, soil – pore fluid behavior of a silo under an earthquake loading is investigated. To predict the response of the silo with the soil surrounding it, '*the linear-elastic constitutive model*' is adopted with soil properties; shear modulus and damping ratio; are strains and cycle independent.

A computer program using dynamic stiffness matrix analyses (DSMA) for predicting and analyzing the model was established using FORTRAN coding. The program is based on geophysical values (such as primary velocity (v_p), shear velocity (v_s), modulus of elasticity (E), mass density (ρ), shear modulus (G),….etc). The values were obtained from field test results for the soil under a silo located in Kirkuk, Iraq.

To check and compare the obtained results, the computer program (MSC/NASTRAN) is used also for predicting and analyzing the same problem. This second program uses input values such as shear modulus (G), modulus of elasticity (E), mass density (ρ) and damping ratio (ζ) obtained from conventional laboratory tests.

From the two aforementioned analyses, comparisons between the results of the relevant two programs are made. Though program "MSC/NASTRAN" visualizes a realistic behavior of the silo under dynamic loading, due to full response results are expressed for each node, the dynamic stiffness matrix analyses program (DSMA) gives only the maximum value for the horizontal and vertical displacements at that node. Despite of that, program DSMA relies on realistic values of geophysical tests obtained from the field directly.

As a conclusion from this study, the soil-structure interaction zone for the silo at Kirkuk under investigation using both analyses show excellent agreement between the results. The agreement in this study turns out to be more than 95% close between the two algorithms. The easiness through which geophysical field tests are conducted, the simplicity of carrying out the required calculations and the reliability of the results makes the dynamic stiffness matrix analysis method (DSMA) highly recommended. It can give an excellent directive about the response of structures resting on soils and subjected to dynamic loads.

Keywords
Earthquake load, response analysis, Iraq soil, geophysical testing, dynamic stiffness matrix, MSC/NASTRAN.

الخلاصة:

لقد تم دراسة تصرف التربة الصلبة مع مائع المسام تحت سايلو معرض لحمل هزة ارضية. لقد تم اعتماد النموذج التكويني المرن الخطي لتوقع استجابة السايلو و التربة المحيطة باستخدام معامل قص و نسبة اخماد غير معتمدين على الانفعالات و الدوران.

لقد تم التحقق من برنامج حاسوبي بالاعتماد على طريقة تحليل مصفوفة الجساءة الحركية لتوقع و تحليل النموذج باستخدام لغة فورتران الحاسوبية. يعتمد البرنامج على قيم جيوفيزيائية (مثل السرعة الاولية و سرعة القص و معامل المرونة و كثافة الكتلة و معامل القص ...الخ). لقد تم الحصول على القيم من نتائج فحص حقلي للتربة تحت السايلو في مدينة كركوك بالعراق.

لقد تم استخدام البرنامج الحاسوبي لتدقيق و مقارنة النتائج المستحصلة عن التحليل السابق مع التوقع و التحليل بطريقة الاستجابة الحركية لنفس المسألة. يستخدم هذا البرنامج الثاني قيم ادخالية مثل معامل القص و معامل المرونة و كثافة الكتلة و نسبة الاخماد مستحصلة عن فحوص مختبرية تقليدية.
من التحليلين المذكورين, تم اجراء مقارنة بين النتائج المستحصلة عن البرنامجين. بالرغم ان البرنامج يعبر عن التصرف الواقعي للسايلو تحت حمل حركي بسبب نتائج الاستجابة الكاملة المستحصلة, يعطي برنامج تحاليل مصفوفة الجساءة الحركية القيم القصوى للازاحتين الافقية و الشاقولية في تلك العقدة. مع ذلك, يعتمد هذا البرنامج على قيم حقيقية عن فحوص جيوفيزيائية مستحصلة من الموقع مباشرة. كنتيجة نهائية عن الدراسة, يظهر توافقاً عالياً بين النتائج المستحصلة عن التحليلين بالنسبة الى منطقة التفاعل المتبادل بين التربة و المنشأ للسايلو في كركوك و بنسبة تقارب تزيد عن 95%. بسبب سهولة اجراء الفحوص الجيوفيزيائية الحقلية و بساطة اجراء الحسابات و دقة النتائج المستحصلة عن طريقة مصفوفة الجساءة الحركية, نقترح اجراءها بشكل مستمر عند التعامل مع هذا النوع من المسائل. بامكان هذه الطريقة ان تعطي تصوراً دقيقاً حول الاستجابة القصوى للمنشأآت الراقدة على الترب و المتعرضة لاحمال حركية.

Introduction

For a satisfactory solution of any soil dynamic problem, one must:

- establish the soil profile, including layering and depth of bedrock, physical characterization and classification of each layer, elevation of water table and ground water conditions and the extent of lateral homogeneity, and
- determine (in the laboratory or in-situ testing) the material parameters of each soil layer needed in the constitutive models to be used in the planned dynamic analysis.

The soil properties that exert the greater influence on the dynamic response of the soil masses and soil-foundation systems are those related to the shearing stress-strain behavior. For small amplitude vibrations including strains ($\gamma < 1/10^5$) in the soil, this behavior is best described through a linear hysteretic model of shear modulus (G_o) and damping ratio (ζ).

(G_o) is the initial slope at the origin of the shearing stress-strain (τ-γ) curve. At large strains ($1/10^5 < \gamma < 1/10^4$), soil behaviour can be best modelled as quasi-linear, described through a secant modulus (G) and a damping ratio (ζ). (G) is a decreasing function of (γ). On the other hand, (ζ) increases with (γ) and may take values up to about 0.07 at $\gamma = 1/10^4$. As strain amplitudes increase beyond ($1/10^4$), nonlinear phenomena become increasingly important.

Testing Techniques

Field Tests

Several types of field tests have been developed to measure shear modulus, damping, and Poisson's ratio. These may include the *cross-borehole propagation method*, the *up-hole and down-hole wave propagation methods* and the *surface wave propagation method*. In this research, results from the first method are obtained and analyzed by the developed theory.

The Cross-Borehole Wave Propagation Method

In the cross-borehole method, the wave propagation velocity from one subsurface boring to a another is measured (Stoke and Woods, 1972).

At least two boreholes are required, one for the impulse and one or more for sensors. This is shown in Figure 1 below:

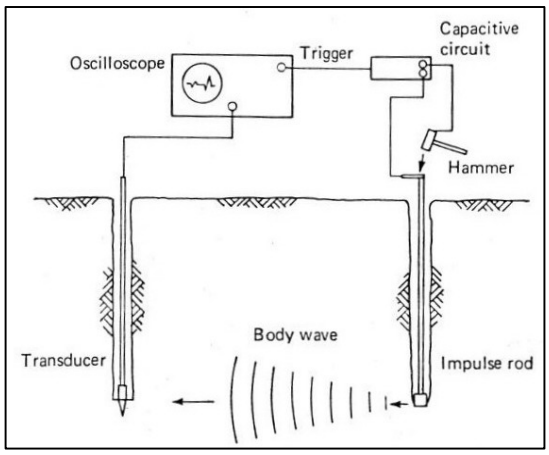

Fig. 1. Cross-borehole method

The impulse rod is struck on top, causing an impulse to travel down the rod to the soil at the bottom of the hole. The shearing between the rod and the soil creates shear waves that travel horizontally through the soil to the vertical motion sensor in the second hole; the time required for a shear wave to traverse this known distance is measured. There are four sources of major concern in conducting cross-borehole shear tests: the borehole, the seismic source, the seismic receiver and the recording and timing equipment.

Although a minimum of two boreholes must always be used, for extensive investigations and for increased accuracy, whenever possible, three or more boreholes are suitable. If boreholes are installed in a straight line, wave velocities can be calculated from the intervals of time required for passage between any two boreholes. Thus, the necessity for precisely recording the triggering time is eliminated. In addition, the boreholes must be vertical to properly measure travel distance. In general, any borehole (10m) or more deep should be surveyed using an inclinometer or another logging device for determining verticality (Woods, 1978).

Although both impulsive and steady-state seismic sources are in use, impulsive sources predominate.

The major criteria for a seismic source are:

- It must be capable of generating predominantly one kind of a wave.
- It must be capable of repeating desired characteristics at a predetermined energy level.

Velocity transducers (geophones) that have natural frequencies of 4 to 15 Hz are adequate for detecting (receiving) the shear waves as they arrive from the source. The receivers must be oriented in the shearing mode and should be securely coupled to the sides of the boring.

Furthermore, the recording equipment should be able to resolve arrival times of up to (0.2) ms or (5) percent of the travel time. Storage oscilloscopes are often used for this as well.

Laboratory Testing Techniques

As in the field, several laboratory devices have been designed to obtain the dynamic properties of the soil. Of the most common tests are the *resonant column*, *ultrasonic pulse*, *cyclic triaxial*, *cyclic simple* shear and cyclic torsional shear tests. Table 1 below shows the dynamic moduli and material damping coefficients obtained from each one of the tests mentioned.

Table(1) Laboratory techniques for measuring dynamic soil properties (Al-Jumaily, 1988).

	Shear modulus	Young's modulus	Material damping
Resonant column	X	X	X
Ultrasonic pulse	X	X	-
Cyclic triaxial	-	X	X
Cyclic simple shear	X	-	X
Cyclic torsional shear	X	-	X

Notation: X indicates that the parameter is determined by the test.

In this paper, only results obtained from field tests are employed to analyze the problems under consideration herein.

ANALYSIS TECHNIQUES

Dynamic Stiffness Matrix Analysis

The dynamic stiffness matrix is described as shown by Equation 1 below. This equation is derived from the equation of motion by which a detailed description can be found in Salih (2005). The form of the equation is as follows:

$$\begin{Bmatrix} P_1 \\ iR_1 \\ P_2 \\ iR_2 \end{Bmatrix} = \frac{(1+t^2)kG^*}{D} \begin{bmatrix} \frac{1}{t}\cos ksd \sin ktd & & & \\ +s \sin ksd \cos ktd & & & \\ \frac{3-t^2}{1+t^2}(1-\cos ksd \cos ktd) & \frac{1}{s}\sin ksd \cos ktd & & \\ +\frac{1+2s^2t^2-t^2}{st(1+t^2)}\sin ksd \sin ktd & +t \cos ksd \sin ktd & & \\ -s \sin ksd & -\cos ksd & \frac{1}{t}\cos ksd \sin ktd & \\ -\frac{1}{t}\sin ktd & +\cos ktd & +s \sin ksd \cos ktd & \\ \cos ksd & -\frac{1}{s}\sin ksd & \frac{t^2-3}{1+t^2}(1-\cos ksd \cos ktd) & \frac{1}{s}\sin ksd \cos ktd \\ -\cos ktd & -t \sin ktd & +\frac{t^2-2s^2t^2-1}{st(1+t^2)}\sin ksd \sin ktd & +t \cos ksd \sin ktdf \end{bmatrix} \begin{Bmatrix} u_1 \\ iw_1 \\ u_2 \\ iw_2 \end{Bmatrix}$$

symmetry

… (1)

where

D=2(1- cos ksd cos ktd)+(st+(1/st)) sin ksd sin ktd

$P_1=-\tau_{xz1}$, $R_1=-\sigma_{z1}$, $P_2=\tau_{xz2}$, and $R_2=\sigma_{z2}$

In the above:

$$\sigma_z(z) = ikl_x(1-t^2)G^*[A_p \exp(iksz) + B_p \exp(-iksz) - i2km_xtG^*[A_{sv} \exp(iktz) - B_{sv} \exp(-iktz)]$$

$$\tau_{xz}(z) = i2kl_xsG^*[A_p \exp(iksz) - B_p \exp(-iksz) + ikm_x(1-t^2)G^*[A_{sv} \exp(iktz) + B_{sv} \exp(-iktz)]$$

In Equation (1), the left part represents the stress effects at the selected depth of layer (d). These stresses are calculated by using the formulations enlisted after Equation 1. These formulations depend on values like (k, l_x, m_x, s, t, …etc.) which are calculated by using equations, depending on properties

of soil (G, μ, ρ, E) obtained by field geophysical tests like the cross borehole method (Wolf, 1985 and Salih, 2005).

The right hand side of Equation (1) consists of two parts:

First: the matrix in which its parameters depend on calculations obtained from values extracted out from geophysical tests such as (G, μ, ρ, E). From these values, the matrix is calculated.

Second: the vector part representing the displacements (both horizontal and vertical) at the top and the bottom of the soil layer. From these displacements, the response of the model can be calculated.

Programming the matrix shown in Equation 1 is done by using a personal computer and FORTRAN language. It is performed in such a way that the user can enter the input values and obtain the output smoothly and directly. The user enters the input values (G, μ, ρ, E, ω) which are obtained from geophysical tests. After that, the program calculates the parameters of the Equation (1) (k, l_x, m_x, s, t, G^*, A_{sv}, C_x, C_y, σ, τ) by using the suitable equations for each parameter. Finally, values of horizontal and vertical displacements are obtained (w and u) and these values represent the output from the program.

TRANSIENT RESPONSE ANALYSIS

Transient response analysis is the most general method used for computing forced dynamic responses. The purpose of a transient response analysis is to compute the behavior of a structure subjected to time-varying excitations. The transient excitation is explicitly defined in the time domain. All of the forces applied to the structure are known at each instant in time. Forces can be in the form of applied forces and/or enforced motions (Clough and Penzien, 1975).

The important results obtained from a transient analysis are typically *displacements*, *velocities*, and *accelerations* of grid points, and forces and stresses in elements.

Depending upon the structure and the nature of the loading, two different numerical methods can be used for a transient response analysis: *direct* and *modal*. The *direct* method performs a numerical integration on the complete coupled equations of motion. The *modal* method utilizes the mode shapes of the structure to reduce and uncouple the equations of motion (when modal or no damping is used); the solution is then obtained through the summation of the individual modal responses. The choice of the approach is problem dependent. The direct method of analysis is performed herein.

Direct Transient Response Analysis

In direct transient response, structural response is computed by solving a set of coupled equations using direct numerical integration. Begin with the dynamic equation of motion in matrix form (Clough and Penzien, 1975):

$$[M] \{ \ddot{X}(t) \} + [C] \{ \dot{X}(t) \} + [K] \{ x(t) \} = \{ P(t) \} \qquad (2)$$

The fundamental structural response (displacement) is solved at discrete times, typically with a fixed integration time step, delta t.

The damping matrix [C] is used to represent the energy dissipation characteristics of a structure. In the general case, the damping matrix is comprised of several matrices which are a function of viscous dampers and equivalent structural damping.

Transient response analysis does not permit the use of complex coefficients. Therefore, structural damping is included by means of equivalent viscous damping. To appreciate the impact of this on the solution, a relation between structural damping and equivalent viscous damping must be defined.

The viscous damping force is a damping force that is a function of a damping coefficient b and the velocity. It is an induced force that is represented in the equation of motion using the [C] matrix and velocity vector.

$$[M] \{ \ddot{X}(t) \} + [C] \{ \dot{X}(t) \} + [K] \{ X(t) \} = \{ P(t) \} \qquad (3)$$

The structural damping force is a displacement-dependent damping. The structural damping force is a function of a damping coefficient G and a complex component of the structural stiffness matrix.

$$[M] \{ \ddot{X} (t)\} + (1 + i G) [K] \{ X (t)\} = \{ P (t) \} \quad (4)$$

Assuming constant amplitude oscillatory response for a single degree-of-freedom system, the two damping forces are identical if:

$$G k = b w \quad (5a)$$

or

$$b = G k / w \quad (5b)$$

Therefore, if structural damping G is to be modelled using equivalent viscous damping b, then the equality holds at only one frequency.

Two parameters are used to convert structural damping to equivalent viscous damping. An overall structural damping coefficient can be applied to the entire system stiffness matrix using the circular frequency (rad/sec) at which damping is to be made equivalent. This parameter is used in conjunction with overall structural damping. The default value for ω_3 is 0.0, which causes the damping related to this source to be ignored in transient analysis.

ω_4 is an alternate parameter used to convert element structural damping to equivalent viscous damping. ω_4 is used in conjunction with structural damping on the material specification. The default value for ω_4 is 0.0 which causes the related damping terms to be ignored in transient analysis.

Units for ω_3 and ω_4 are radians per unit time. The choice of ω_3 or ω_4 is typically the dominant frequency at which the damping is active. Often, the first natural frequency is chosen, but isolated individual element damping can occur at different frequencies and can be handled by the appropriate data entries.

Version 4.4 Of Program "Msc/Nastran

The dynamic response option of MSC/NASTRAN for Windows consists of the following capabilities:

A. *Frequency response* which computes the steady-state response to a sinusoidal excitation.

B. *Transient response* which computes the response to a general, time-varying excitation.

In this paper, only transient analysis is employed with Newmark's integration (Salih, 2005).

Verification Problem

In this paper, the effect of dynamic loads on a structure and its surrounding soil is considered. Figure (2) shows a concrete structure resting on a soil medium. The analysis will be conducted on the concrete member alone first, then on the soil medium alone and on the combined soil structure system later. Analyses of results are done by two algorithms:

*. The dynamic stiffness matrix analysis (DSMA) which depends on geophysical test results.

**. MSC/NASTRAN analysis.

After that, comparisons between these two algorithms are made.

Earthquake Loading

The El-Centro earthquake is applied. This earthquake was recorded at a site in El-Centro, California during the Imperial Valley, California earthquake of May 18, 1940. A digital form including 1559 data points covering 31.16 seconds with an intensity of (0.15g) is input to the programs (Chopra, 1996). The selected time step is 0.05 seconds. It is used to investigate the behavior of soil-structure interaction under earthquake loads. The chosen magnitude of this earthquake on the Richter scale is (4.5).

Modelling The Problem

A. Soil medium alone: At first, the soil medium is taken alone under the earthquake load. This model is 29 meters long, 1 meter wide and 6 meters high. Its properties are given in Table (2).

Table(2). Material Properties for Soil Model.

Unit weight (γ_s)	19.80 kN/m^3
Elasticity modulus (E)	150000 kN/m^2
Poisons ratio (μ)	0.397
Damping ratio (ζ)	0.05

The above presented values are obtained from geophysical tests (cross borehole method) conducted by the National Center for Construction Laboratories and Research.
A selected node was taken to show the response of the soil model under earthquake load.

B. Concrete model alone: The selected earthquake is applied then onto the concrete model alone. The concrete model is 5 meters long, 0.25 meters wide and 0.3 meters high. Its properties are as follows:

Table(3). Material properties of concrete model.

Unit weight (γ_c)	24.00 kN/m^3
Elasticity modulus (E)	23500000 kN/m^2
Poisons ratio (μ)	0.3
Damping ratio (ζ)	0.05

Again, a selected node was taken into consideration to show the response of the concrete model under earthquake load.

C. Combined concrete resting on soil medium: Finally, the earthquake load is applied to the base of the model (structure and soil) with properties as follows:

Table(4) Combined problem material properties.

	Structure	Soil
Unit weight (γ_s) kN/m^3	24.00	19.80
Elasticity modulus (E) kN/m^2	23500000	150000
Poisons ratio (μ)	0.3	0.397
Damping ratio (ζ)	0.05	0.05

Node (754) (as shown in Figure 2) is taken as a representative point to study the response of the whole model under the dynamic load.

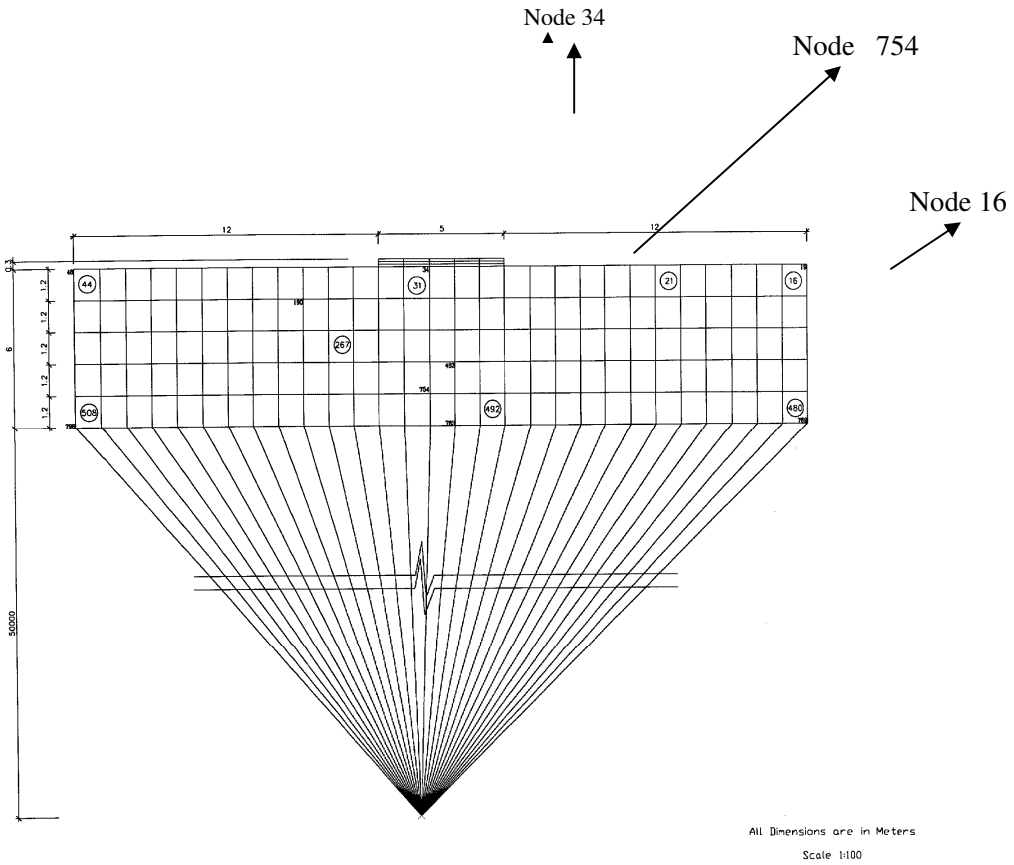

Figure 2 Front view of soil-structure interaction**.**

Dynamic Stiffness Matrix Analyses Program (DSMA)

The results obtained from DSMA are shown below. The input data for this program are taken from the geophysical tests (cross borehole method) conducted by the National Centre for Construction Laboratories and Research.

Displacements At node (754) Using (DSMA)

1. The given values (obtained from The National Centre for Construction Laboratories and Research) are listed in Table (5) below.

Table(5) Geophysical Test Results (4.8 m) depth*.

ζ_s	ζ_p	Depth (m)	ω (Hz)	μ	E (kN/m^2)	G (kN/m^2)	P (kN/m3)	A_p	B_p	V_s (m/sec.)
0.05	0.05	4.8	10	0.373	$2.2*10^8$	$1.8*10^8$	1.98	0.13	0.13	378

* Every parameter in this table is described in the list of symbols.

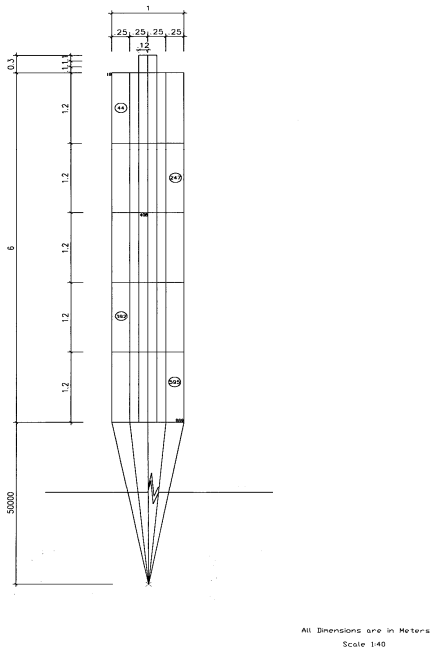

Figure 3 Side view of soil-structure model.

2. Calculation obtained by the program:
Assume $\theta_s=20^{\circ}$
$\theta_p=11.31$ $l_x=0.981$ $m_x=0.9397$ $m_y=0.342$ $C_x=355.2$ $C_y=129.28$ $S=0.1978$ $t=0.3639$
$K=4.508*10^{-4} - 2.248*10^{-5}$ i $G^*=2.7*10^8 + 2.7*10^7$ i $A_{sv} = B_{sv} = -0.1716$
$\sigma = - 1.378*10^3 + 2.7066*10^5$ i $\tau = 1.7*10^3 - 3.42*10^4$ i
3. Displacements for this node:
Horizontal displacement=-0.13m Vertical displacement =0.58m

It can be observed from displacements obtained that the maximum displacements have values of (13) cm horizontal and (58) cm vertical.

The calculated displacements are out of the range of allowable displacements according to the Iraqi code (Building Research Center, 1997) which is h/600; in which h = is the height of the building. Furthermore, the height of the model is 0.3 meters; therefore, 0.3/600 = 0.0005m. Hence, the displacements are out of the allowable displacement range.

Msc/Nastran Algorithm Solution

A-Soil Model Alone

A 6-meter-high by 29 meter in length and 1 meter in thickness soil medium is modeled using 8-noded three-dimensional finite elements as shown in Figures 4 and 5. Nodes at the top and the bottom of the model are selected (node 16 and node 766 as shown in Figure 4) to find the response and magnitude of displacements under an El Centro earthquake load. The nodes along the boundaries of the mesh are restrained against horizontal and vertical movements. The properties of the soil are given in Table (6) below.

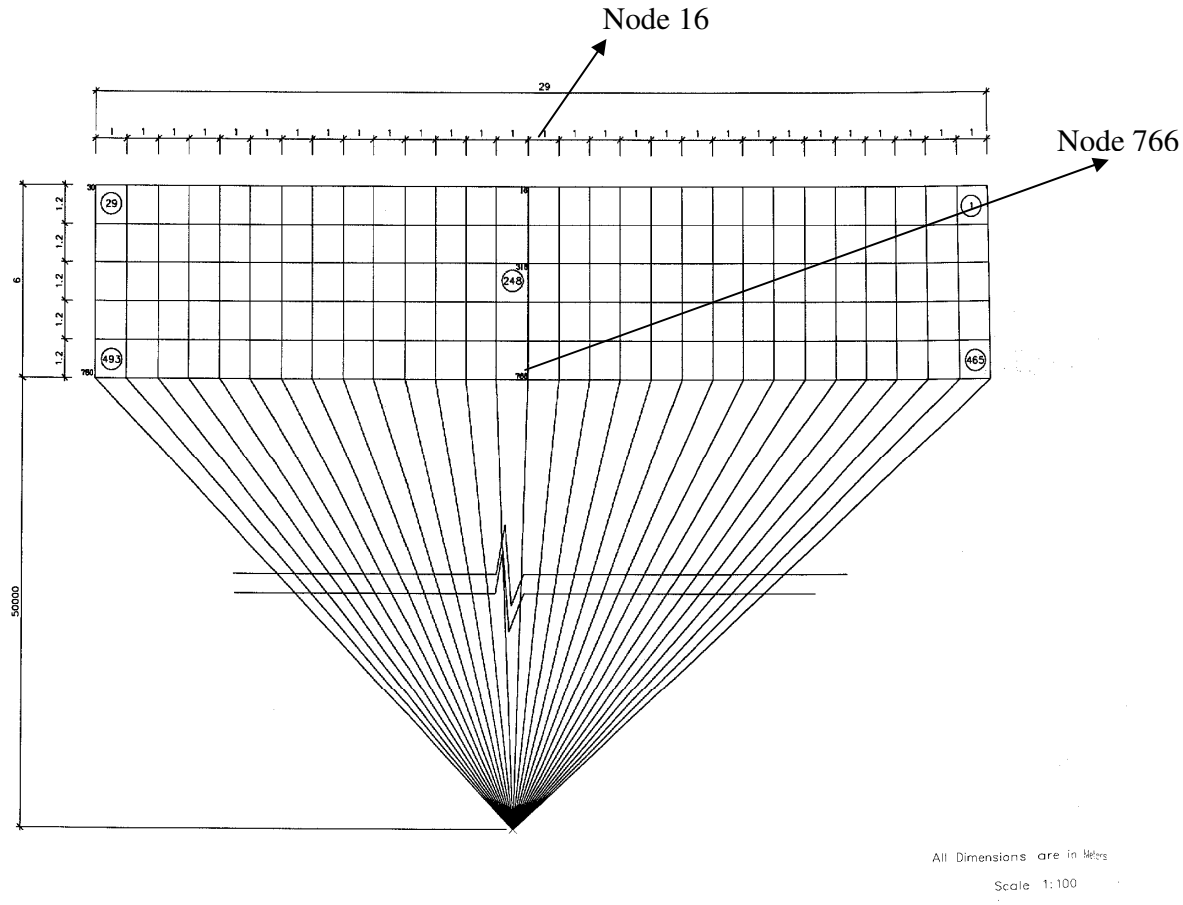

Figure 4 Front view of soil model.

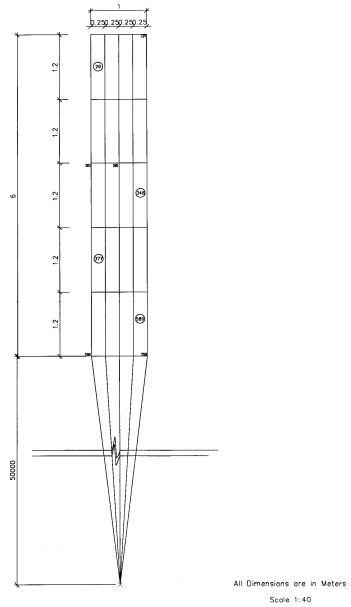

Figure 5 Side view of soil model.

Table(6. Soil properties.

Unit weight (γ_s)	19.80 (kN/m^3)
Elasticity modulus (E)	150000 (kN/m^2)
Poisson's ratio (μ)	0.397
Damping ratio (ζ)	0.05

Figures (6) and (7) show the displacements at selected nodes.

Maximum Displacement = 0.3 m

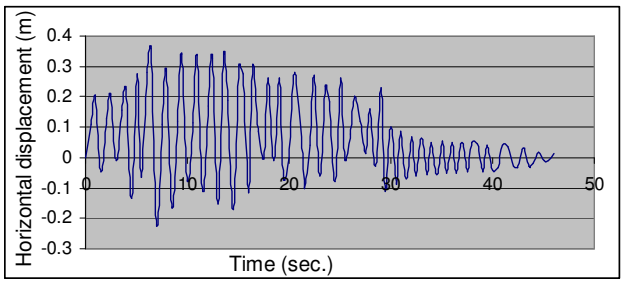

Maximum Displacement = 0.53 m

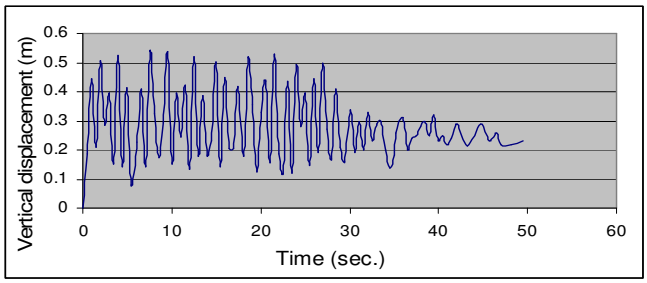

Fig(6). The displacement response at the top of the soil model (node 16) in Figure 2.

Maximum Displacement = 0.13 m

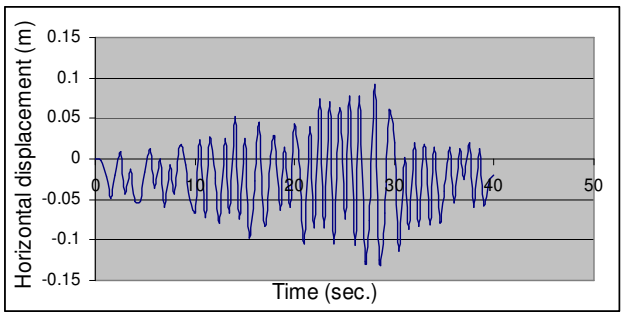

Maximum Displacement = 0.57 m

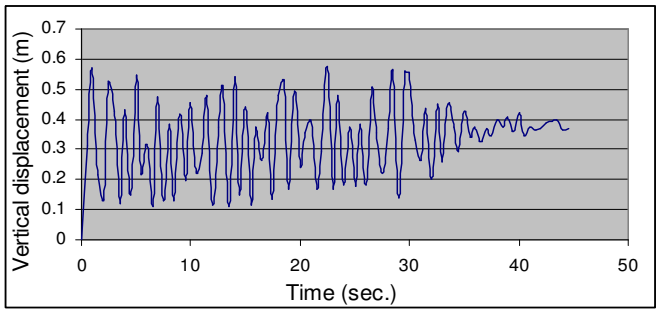

Fig(7). The displacement response at the base of the soil model (node 766) in Figure 2.

It can be observed from the displacements figures that the maximum displacements have values of (0.36) m horizontal and (0.57) m vertical.
Also, displacements decrease with time due to damping.

B-The Concrete Model Alone

An 0.3 meter high, 5 meters long and 0.25 meter wide concrete wall is modeled by the three dimensional finite element mesh of the serendipity type as shown in Figures 8a and b.

In this model, 8-noded elements are used to represent the wall in the finite element mesh. The nodes along the right and left boundaries of the mesh are restrained against vertical and horizontal movements.

The choice of points are made at the top and the base of the wall (node 21 and node 3 as shown in Figure 8) to show the response of these nodes when an El Centro earthquake excitation is applied to that wall of an intensity of 4.5 on the Richter scale..

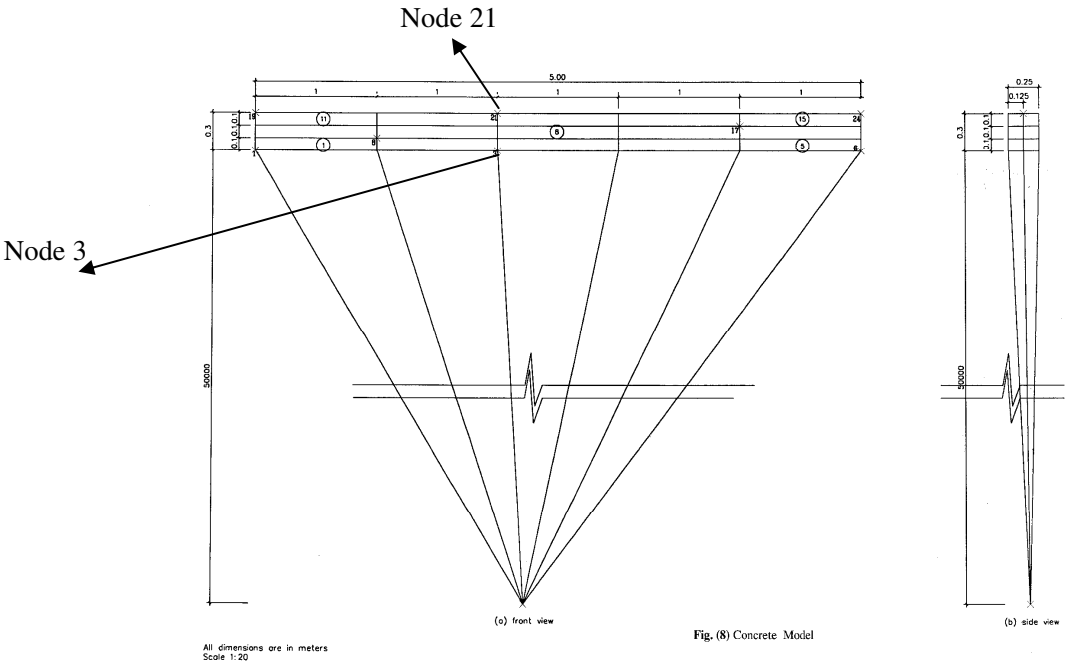

Fig (8). The concrete model alone.

The properties of the concrete wall are given in Table (7).

Table(7) Concrete wall properties

Unit weight (γ_c)	24.00 (kN/m^3)
Elasticity modulus (E)	23500000 (kN/m^2)
Poisson's ratio (μ)	0.3
Damping ratio (ζ)	0.05

Figs (9). and (10) show the results of displacements at selected nodes in the wall.

Maximum Displacement = 0.28 m

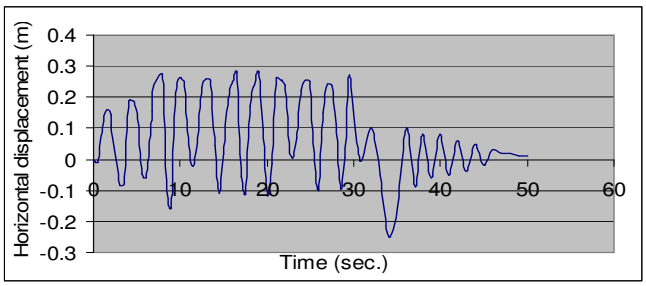

Maximum Displacement = 0.58 m

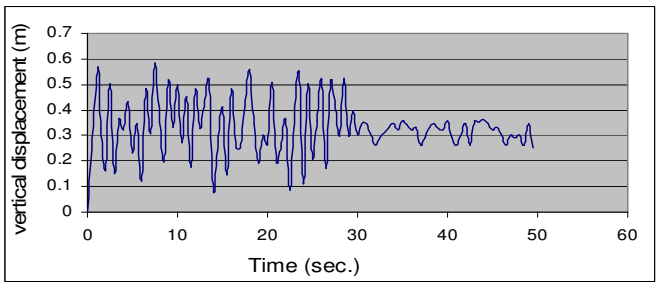

Fig(9). The displacement response at the top of the concrete wall (node 21) in Fig 6a.

Maximum Displacement = 0.5 m

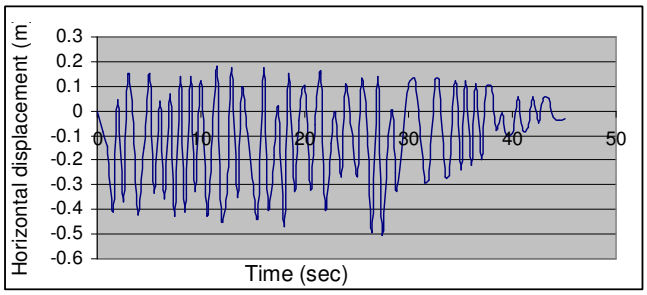

Maximum Displacement = 0.66 m

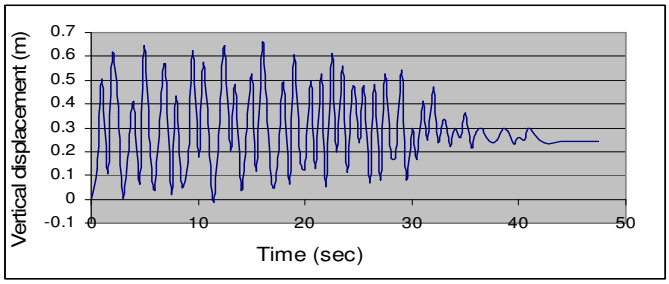

Fig(10). The displacement response at the base of the concrete wall (node 3) in Figure 6a.

It can be observed from displacements figures that the maximum displacements have values of (0.50) m horizontal and (0.66) m vertical.
Also, displacements decrease with time due to damping.

The calculated displacements are out of range of the allowable displacements according to the Iraqi code (Building Research Center, 1997) which is h/600; in which h = is the height of the building. Also, the height of the silo is 0.3 meters. Hence, 0.3/600 = 0.0005 meter which implies that the displacements are out of the allowable range.

C-Soil-Structure (Concrete) Interaction Model

In this model; the interaction between structure (concrete) and soil is studied according to what is shown in Figures (2) and (3). Again, the earthquake load adopted is the El-Centro earthquake excitation. This load is subjected to the model. The properties of the soil and the concrete wall are the same as depicted in Tables (6) and (7) and gathered in Table (8) below.

In this model, 8-noded three dimensional elements are used to represent the problem in the finite element mesh (Figures (2) and (3)). The nodes along the right and left boundaries of the mesh are restrained against vertical and horizontal movements.

After that, the displacements at the interaction nodes are calculated such as node number 34 shown in Figure (2). Figure (11) shows the displacements for this node against time.

Table (8) Material properties

Property	Concrete	Soil
Unit weight (γ) (kN/m^3)	24.00	19.80
Elasticity modulus (E) (kN/m^2)	23500000	150000
Poisson's ratio (μ)	0.3	0.397
Damping ratio (ζ)	0.05	0.05

Maximum Displacement = 0.2 m

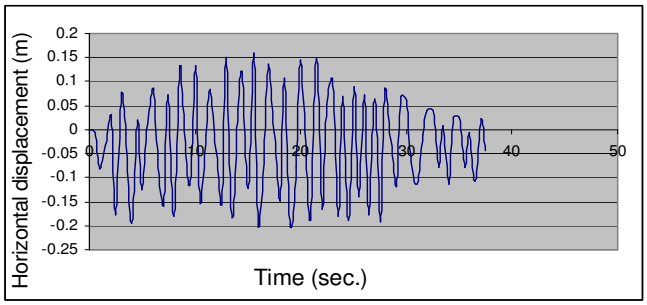

Maximum Displacement = 0.53 m

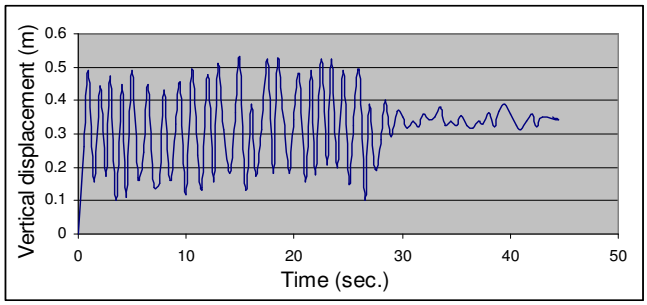

Fig(11). The displacement response at node (34) in Figure 2.

It can be observed from the displacements figures that the maximum displacements have values of (0.2) m horizontal and (0.53) m vertical. Also, displacements decrease with time due to damping.

The calculated displacements are out of range of the allowable displacements according to the Iraqi code (Building Research Center, 1997) which is h/600; in which h = is the height of the building. Also, the height of the model is 0.3 meters. Hence, 0.3/600 = 0.0005 meter. Therefore, the displacements are out of the allowable displacement range.

From Figure (2), node 754 is chosen to find the displacements of it and to further check these displacements with those obtained from (DSMA) program. These displacements are presented in Figure (12).

Maximum Displacement = -0.13 m

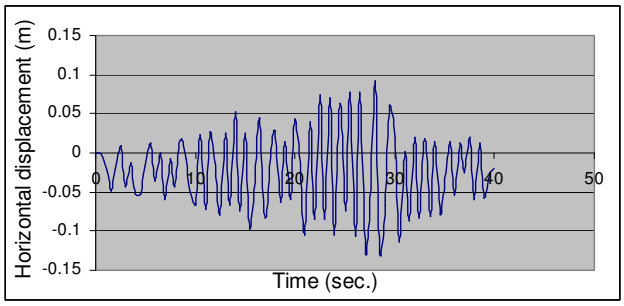

Maximum Displacement = 0.58 m

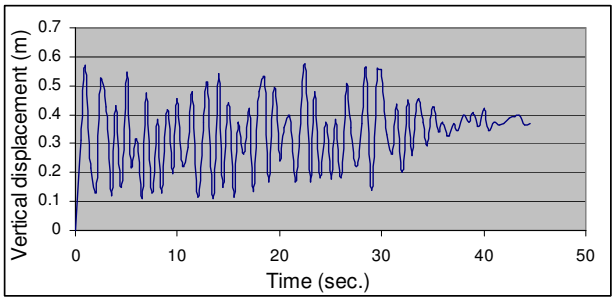

Fig(12). The displacement response at the base of the soil-structure model (node 754) in Figure 2.

Comparison of Results and Verification

Finally, Table (9) compares the results from the two algorithms presented for nodal point (754) as shown in Fig (2).

Table(9) Comparison of results from the two algorithms for node (754) as shown in Figure 2.

Program	Node No.	Horizontal displacement (m)	Vertical displacement (m)
DSMA	754	-0.128	0.576
NASTRAN	754	-0.13	0.58

Table (10) below depicts that only a small deviation is encountered when using the two algorithms under consideration. This gives confidence on the results obtained by the dynamic stiffness matrix analysis (DSMA) method which relies on geophysical test results.

Table(10). Comparison between DSMA and MSC/NASTRAN.

Node No.	Ratio (DSMA / (MSC/NASTRAN))	
	Horizontal displacement (%)	Vertical displacement (%)
754	98.4	99.3

After establishing confidence on the results obtained by program DSMA, the forthcoming section presents an analysis of a realistic problem (a concrete silo resting on a clayey soil) by using both methods.

Problem Description: Case Study (Kirkuk Silo)

In this study, the effect of earthquake load on a certain structure in Iraq (a silo in Kirkuk) is taken into consideration. Kirkuk silo lies in Al-Ta'meem governorate to the north of the middle of Iraq. Kirkuk silo is a concrete structure for storing grain materials. Its dimensions are (62.8) meters long, (17.6) meters wide and (45) meters high (Figures 13 and 14). The soil under the silo is a clayey one.

Figure (15) shows the contact zone between the concrete silo and the soil medium. The properties of concrete and soil are shown in Table (11). The properties of soil are defined from geophysical tests conducted by The National Center for Construction Laboratories and Research. The geophysical method employed for these tests is the cross borehole one. The applied earthquake is the El-Centro earthquake with an intensity of (0.15g). This earthquake is applied to the base of the model. After the material properties were obtained, the analyses were done by the two algorithms:-

1. Dynamic-stiffness matrix analyses (DSMA).
2. MSC/NASTRAN program analysis.

Finally, the discussion of the results obtained from these two algorithms is presented.

Table(11) Properties of concrete and soil.

Property	Concrete	Soil
Unit weight (kN/m^3)	24.00	19.80
Elasticity modulus (kN/m^2)	23500000	150000
Poisson's ratio	0.3	0.397
Damping ratio	0.05	0.05

The model shown in Figures (13) and (14), where three-dimensional eight node elements are used, is subjected to this earthquake load.

(DSMA) Program:

1- Displacements at depth (8.33 m) from ground surface (node 637 in Figure 15):

1. The given values from geophysical test results (obtained from the National Centre for Construction Laboratories and Research) are presented in Table (12).

Table(12) Geophysical Tests Results (8.33 m) depth*

ζ_s	ζ_p	Depth(m)	ω (Hz)	μ	E (kN/m^2)	G(kN/m^2)	ρ	A_p	B_p	V_s (m/sec.)
0.05	0.05	8.33	10	0.397	$1.5*10^8$	$1.3*10^8$	1.98	0.58	0.58	353

* Parameters in this table are all defined in the list of symbols.

.Calculations adopted for the program:

Assume $\theta_s=20^\circ$

$\theta_p=3.08$ $l_x=0.998$ $m_x=0.9397$ $m_y=0.342$ $C_x=331.711$ $C_y=120.733$ $S=0.1425$ $t = 0.3663$
$K=3.65*10^{-4} - 1.822*10^{-5}$ i $G^*=4*10^8 + 4*10^7$ i $A_{sv} = B_{sv} = 0.0076$ $\sigma = - 6.87*10^3 + 1.388*10^5$ i
$\tau = - 4.39*10^3 + 8.66*10^4$ i

3. Displacements for this node:
Horizontal displacement=-0.12m Vertical displacement =0.56m

-Displacements at depth (8.33 m) from ground surface (node 666 in Figure 15)

1. The given values from geophysical test results (obtained from the National Centre for Construction Laboratories and Research) are the same as those presented in Table (12).

. Calculations adopted for the program:

Assume $\theta_s=20^\circ$

$\theta_p=9.46$ $l_x=0.986$ $m_x=0.9397$ $m_y=0.342$ $C_x=331.711$ $C_y=120.733$ $S=0.1691$ $t = 0.3639$
$K=6.396*10^{-4} - 3.19*10^{-5}$ i $G^*=1.3*10^8 + 1.3*10^7$ i $A_{sv} = B_{sv} = 0.0076$

$\sigma = - 5.91*10^3 + 1.186*10^5$ i $\tau = - 70.68 + 1.03*10^3$ i

3. Displacements for this node:

Horizontal displacement=0.173m Vertical displacement =0.48m

-Displacements at depth (8.33 m) from ground surface (node 642 in Figure 15)

1. The given values from geophysical test results (obtained from the National Centre for Construction Laboratories and Research) are the same as those presented in Table (12).

. Calculations adopted for the program:

Assume $\theta_s=20^{\circ}$

$\theta_p=5.1$ $l_x=0.996$ $m_x=0.9397$ $m_y=0.342$ $C_x=331.711$ $C_y=120.733$ $S=0.0897$

$t = 0.3639$ $K=6.461*10^{-4} - 3.22*10^{-5}$ i $G^*=1.3*10^8 + 1.3*10^7$ i $A_{sv} = B_{sv} = 0.0076$

$\sigma = - 6.038*10^3 + 1.21*10^5$ i $\tau = - 50.95+ 1.048*10^3$ i

Displacements for this node:

Horizontal displacement=-0.208m Vertical displacement =-0.3m

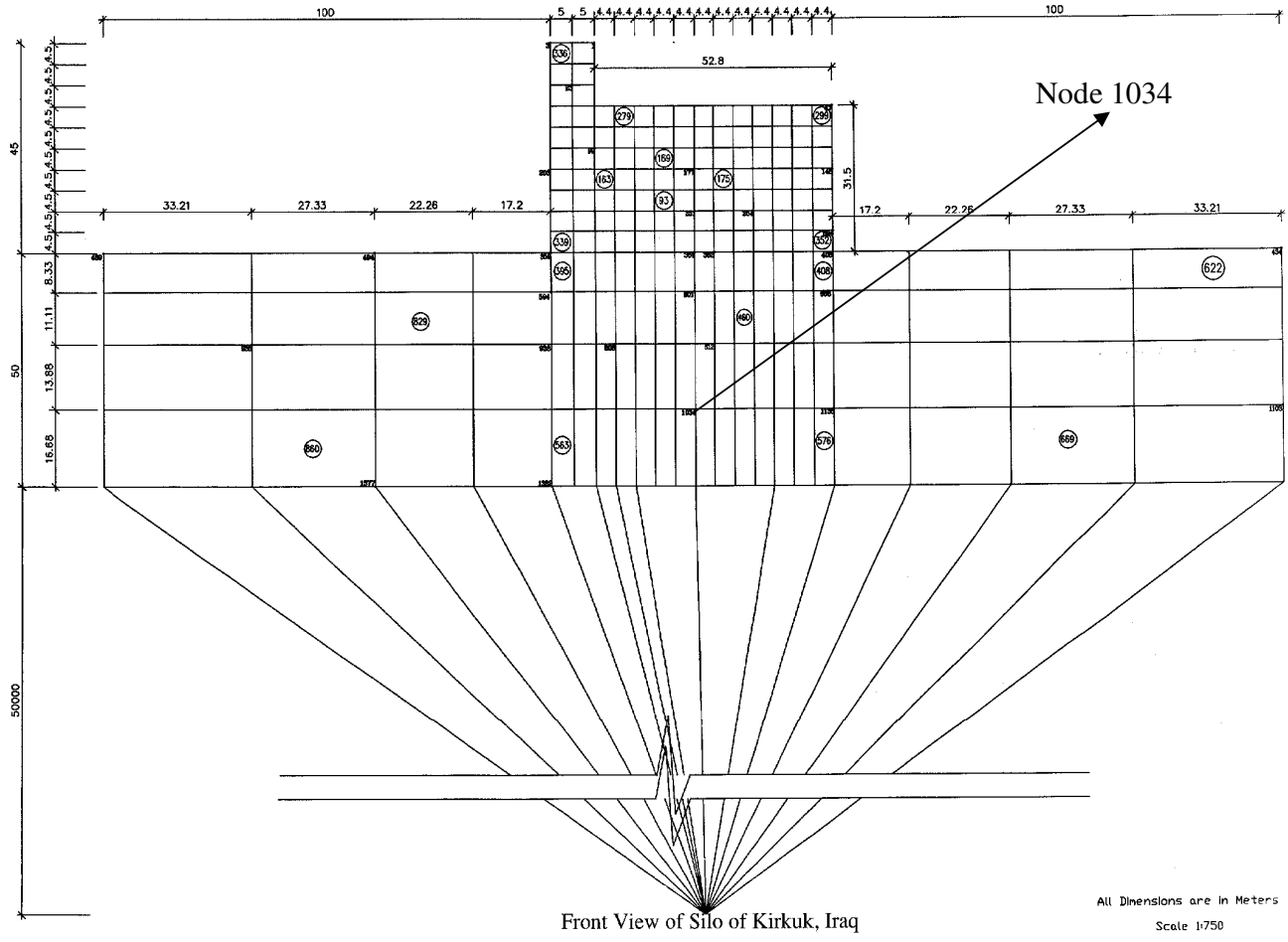

Fig(13). Front view of silo.

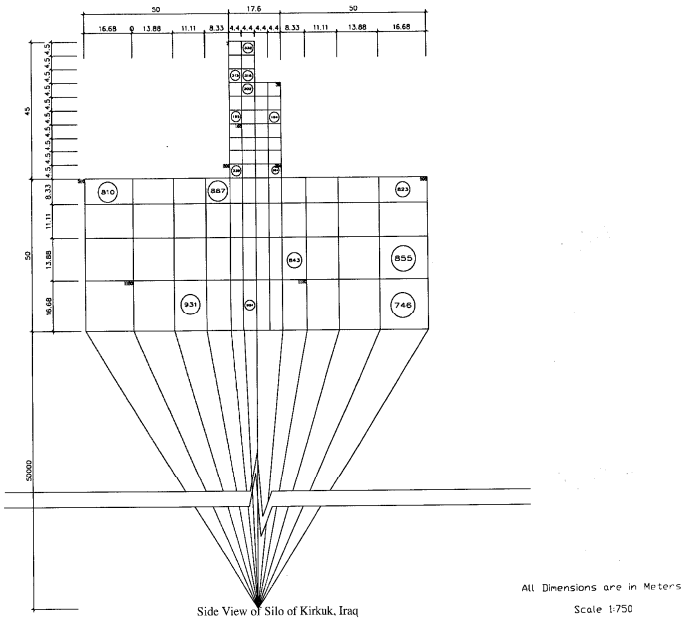

Fig(14). Side view of silo.

-Displacement at depth (33.32 m) from ground surface (node 1034 in Figure 13)

1. The given values from geophysical test results (obtained from the National Centre for Construction Laboratories and Research) are presented in Table (13).

Table(13). Geophysical Tests Results (33.32 m) depth*.

ζ_s	ζ_p	Depth(m)	ω (Hz)	μ	E (kN/m^2)	G(kN/m^2)	P (kN/m3)	A_p	B_p	V_s (m/sec.)
0.05	0.05	33.32	10	0.422	$6.7*10^8$	$5.8*10^8$	2.1	0.58	0.58	582

* Parameters appearing in this table are all defined in the list of symbols

. Calculations adopted for the program:

Assume $\theta_s=25^\circ$

$\theta_p=28.957$ $l_x=0.874$ $m_x=0.906$ $m_y=0.422$ $C_x=527.47$ $C_y=245.96$ $S=1.108$

$t = 0.3663$ $K=1.96*10^{-4} - 9.77*10^{-6}$ i $G^*=5.8*10^8 + 5.8*10^7$ i $A_{sv} = B_{sv} = 0.2476$

$\sigma = - 7.07*10^3 + 1.435*10^5$ i $\tau = - 4.869*10^3 + 4.438*10^4$ i

Displacements for this node:

Horizontal displacement=-0.127m Vertical displacement =0.327m

- Displacement at depth (8.33 m) from ground surface (node 781 in Figure 15)

1. The given values from geophysical test results (obtained from the National Centre for Construction Laboratories and Research) are the same as those presented in Table (12).

. Calculations adopted for the program:

Assume $\theta_s=20^\circ$

$\theta_p=3.039$ $l_x=0.998$ $m_x=0.9397$ $m_y=0.342$ $C_x=331.711$ $C_y=120.733$ $S=0.1425$

$t = 0.3663$ $K=3.653*10^{-4} - 1.8219*10^{-5}$ i $G^*=4*10^8 + 4*10^7$ i $A_{sv} = B_{sv} = 0.0076$

$\sigma = - 6.897*10^3 + 1.373*10^5$ i $\tau = - 4.154*10^3 + 8.4827*10^4$ i

3. Displacements for this node:

Horizontal displacement=-0.255m Vertical displacement =0.575m

Program Msc/Nastran Version 4.4

The same concrete silo in Kirkuk is discretized using three-dimensional finite elements. The model and its dimensions are shown in Figures (13) and (14) while Figure (15) shows the interaction zone of the model.

The nodes at the top, bottom and interaction area are taken to find the displacements when the El-Centro earthquake excitation is subjected to the base of the model. The properties for concrete and soil are listed in Table (11).

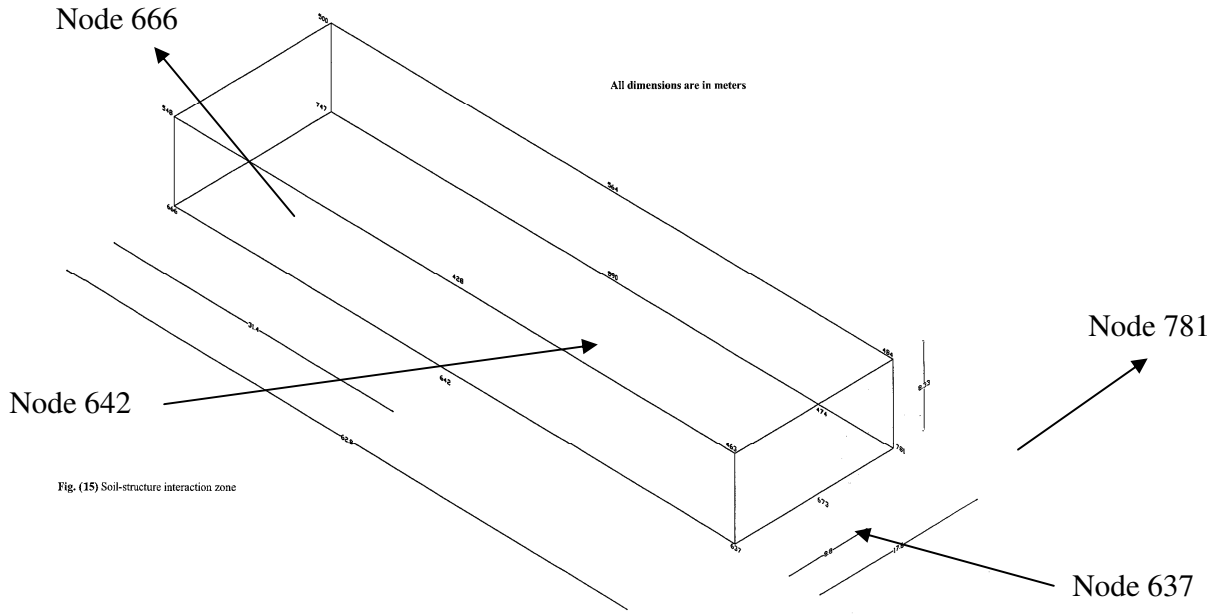

Fig(15). Soil-structure interaction zone.

In this model, 8-noded three-dimensional finite elements are used. The nodes along the boundaries of the mesh are restrained against horizontal and vertical movements.

Maximum Displacement = 0.125 m

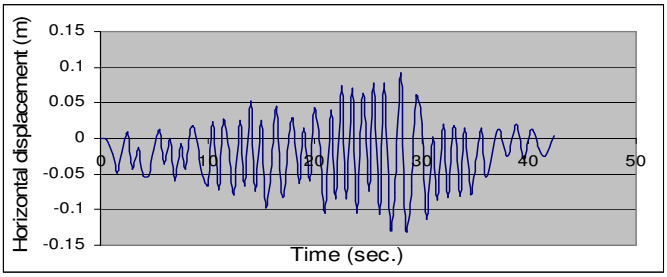

Maximum Displacement = 0.57 m

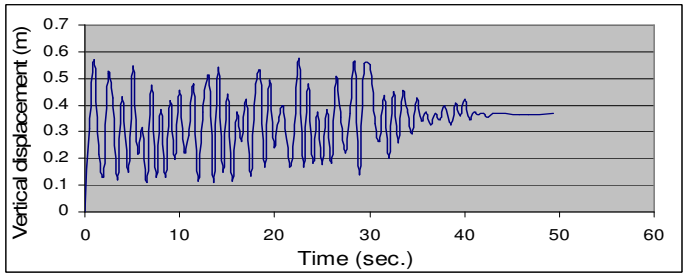

Fig(16). The displacement response at node 637 in Figure 15.

It can be observed from the displacements figures (Figure 16) that the maximum displacements have values of (0.125) m horizontal and (0.57) m vertical. Furthermore, displacements decrease with time due to damping.

The calculated horizontal displacement is out of range of the allowable displacements according to the Iraqi code (Building Research Center, 1997) which is h/600; in which h = is the height of the building. The height of the silo is 45 meters. Therefore, 45/600 = 0.075 meters. Hence, the displacement is out of the allowable range.

It can be observed from the displacements figures (Figure 17) that the maximum displacements

Maximum Displacement = 0.26 m

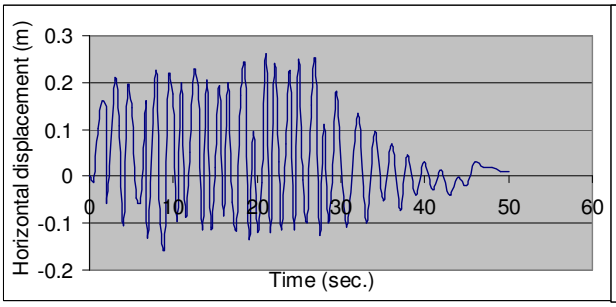

Maximum Displacement = 0.58 m

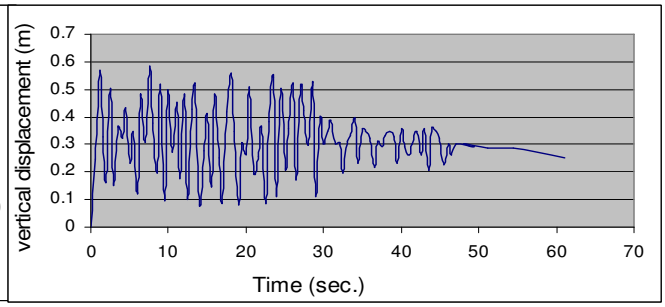

Fig(17). The Displacement Response at node 781 in Figure 15.

have values of (0.26) m horizontal and (0.58) m vertical. Furthermore, displacements decrease with time due to damping.

Again, the displacement is out of the allowable range specified by the Iraqi code.

Maximum Displacement = 0.125 m

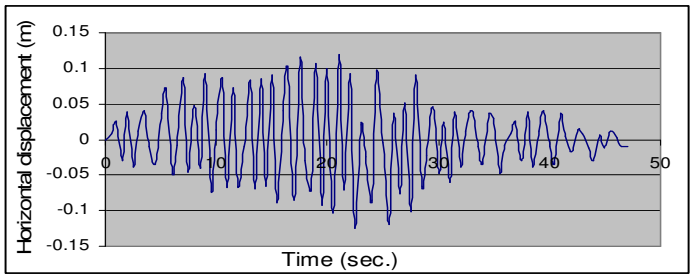

Maximum Displacement = 0.33 m

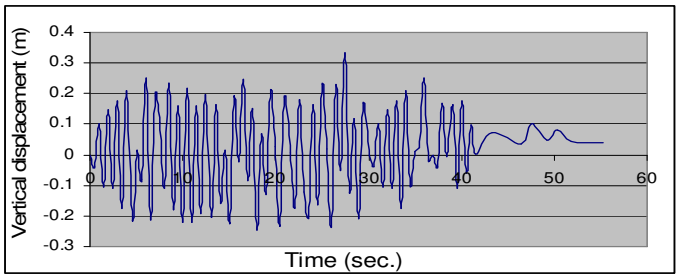

Fig(18). The Displacement Response at node 1034 in Figure 13.

It can be observed from the displacements figures (Figure 18) that the maximum displacements have values of (0.125) m horizontal and (0.33) m vertical. Furthermore, displacements decrease with time due to damping.

Again, the displacement is out of the allowable range specified by the Iraqi code.

Maximum Displacement = 0.175 m

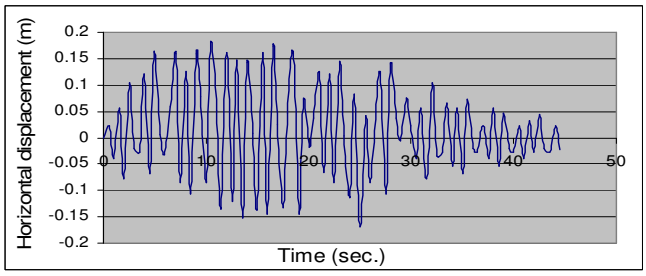

Maximum Displacement = 0.48 m

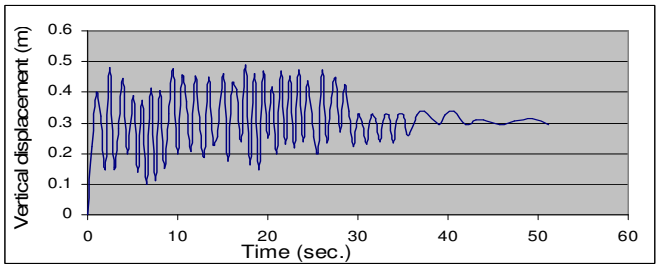

Fig(9). The Displacement Response at node 666 in Figure 15.

It can be observed from the displacements figures (Fig.19) that the maximum displacements have values of (0.175) m horizontal and (0.48) m vertical. Furthermore, displacements decrease with time due to damping.

Again, the displacement is out of the allowable range specified by the Iraqi code.

It can be observed from the displacements figures (Figure 20) that the maximum displacements have values of (0.21) m horizontal and (0.306) m vertical. Furthermore, displacements decrease with time due to damping.

Again, the displacement is out of the allowable range specified by the Iraqi code.

Maximum Displacement = 0.21 m

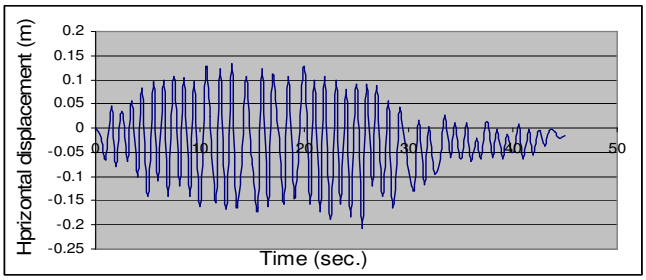

Maximum Displacement = 0.306 m

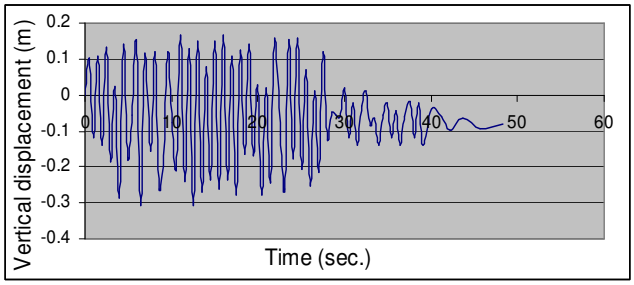

Fig(20). The Displacement Response at node 642 in Figure 15.

Comparison of Results

Tables (14) and (15) below show the comparison of the results of the displacements obtained by the two methods. As can be seen, very close results are obtained.

CONCLUSIONS

The dynamic stiffness method of analysis depends on results obtained from field geophysical tests. A computer program coded in FORTRAN language, namely DSMA, was developed. To assure the reliability of the results obtained from this program, the MSC/NASTRAN Version 4.4 algorithm was adopted from literature for comparison purposes. A verification problem was analyzed first by the two methods. Later on, a realistic structure was considered for analysis purposes. The structure being a concrete silo in Kirkuk, Iraq subjected to an El-Centro earthquake excitation of magnitude of 4.5 on the Richter scale. From the analyses conducted, the following conclusions have been reached:-

1/ By using the method of analysis which relies on geophysical testing (DSMA), it gives results very close to those obtained by the direct integration dynamic finite element method (MSC/NASTRAN).

2/ The deviation in results between the two algorithms is small as shown in Table (15) below.

3/ As presented in the results, the finite element method (MSC/NASTRAN) is more flexible in showing the response of each node in the model under dynamic loads when calculating the vertical and horizontal displacements at that node. On the other hand, (DSMA) gives the displacements only at the surface of contact between the two adjacent layers. However, geophysical tests are much simpler to conduct in the field than conventional testing procedures and results of maximum displacements can be obtained with confidence rapidly.

4/ At any rate, both algorithms show that the structure will render unstable when using both methods of analysis. The load applied is of an expected magnitude in the region. Therefore, it is necessary to study means of converting the structure into a safe one by a separate study. This study also shows the importance of abiding by codes and their provisions, the Iraqi code in this case, when designing structures.

Table(14). Comparison between the two algorithms for horizontal and vertical displacements

Node No.	D.S.M.A		MSC/NASTRAN	
	Horizontal displacement (m)	Vertical displacement (m)	Horizontal displacement (m)	Vertical displacement (m)
637	-0.12	0.56	-0.125	0.57
781	0.225	0.575	0.26	0.58
1034	-0.127	0.327	-0.125	0.33
666	0.173	0.48	0.175	0.48
642	-0.208	-0.3	-0.21	-0.306

Table(15). Comparison of Results between DSMA and MSC/NASTRAN Algorithms

Node No.	Ratio of (DSMA / (MSC/NASTRAN)) Results	
	Horizontal displacement (%)	Vertical displacement (%)
637	96	98.2
781	99.5	99.1
1034	98.4	99
666	98.8	100
642	99	98
Average	98.34	98.86

The adoption of damping in finite element analyses decays away the results of displacements with time.

The easiness through which geophysical field tests are conducted, the simplicity of carrying out the required calculations and the reliability of the results makes the dynamic stiffness matrix analysis method (DSMA) highly recommended. It can give an excellent directive about the response of structures resting on soils and subjected to dynamic loads.

Acknowledgments

The authors wish to note the scientific support of the National Centre for Construction Laboratories and Research of the Ministry of Construction and Housing of Iraq for their scientific support of this study. A special mention has to be made here for the late Mr Issam Saeed from the Centre for his encouragement and enthusiasm.

REFERENCES

- Al-Jumaily, F.A., "Design of Foundations Subjected to Dynamic Loading", Iraqi Society of Engineers, Continuing Education, College of Engineering, University of Baghdad, 1988.
- Building Research Centre, General Commission for Industrial Research and Development, Ministry of Industry and Minerals in Iraq, “Iraqi Seismic Code Requirement for Buildings” Code 2, 1997.
- Chopra A.K.,, "Dynamics of Structures-Theory and Applications to Earthquake Engineering", Prentice-Hall, 1996.
- Clough, R. W. and J. Penzien, "Dynamics of Structures", McGraw-Hill Inc., 1975.
- Salih, M.M., "Dynamic Stiffness Matrix Analysis of Soil-Structure Interaction With Application to a Silo in Kirkuk", MSC Thesis, Department of Civil Engineering, University of Baghdad, 2005.
- Stoke K.H., and R.D. Woods, "In Situ Shear Wave Velocity by Cross-Hole Method”, Journal of Soil Mechanics and Foundation Division, ASCE, Vol. 98 No.SM5, PP.443-460, 1972.
- Wolf, J.P. "Dynamic Soil-Structure Interaction", Prentice Hall, Englewood Cliffs, N.J., 1985.
- Woods, R.D. "Measurement of Dynamic Soil Properties-State of the Art," Proceedings ASCE Specialty Conference on Earthquake Engineering and Soil Dynamics, Pasadena, June 1978.

List of Symbols

A_P Amplitude of a wave whose displacement vector cosincides with the direction of propagation
A_{SH} Amplitude of the horizontal component of the displacement vector of the S-wave
A_{SV} Amplitude of the vertical component of the displacement vector of the S-wave
b Constant of integration
[B] Damping matrix
[C] Damping matrix
C_x Component of Phase velocity in x-direction
C_y Component of Phase velocity in y-direction
d Depth of the selected layer
E Modulus of elasticity
E The amount of earthquake energy released

G	Shear modulus
G_0	Initial slope at the origin of the shearing stress-strain curve
[k]	Static stiffness matrix
K	Wave number
L_x	The scalar which may be considered as the direction cosines of a straight line in x-direction
[M]	Mass matrix
m_x	The direction of propagation in x-direction
m_y	The direction of propagation in y-direction
P	Primary wave
[S]	Dynamic-stiffness matrix
s	Distance between geophones
t	Time
u	Amplitude of horizontal displacement
v_c	Compression wave velocity
v_s	Shear wave velocity
X	Displacement
w	Amplitude of vertical displacement
$\dot{x}$	Velocity
$\ddot{x}$	Acceleration
γ	Shearing stress-strain
ζ	Damping ratio
θ_p	Angle of inclination in primary wave
θ_s	Angle of inclination in share wave
μ	Poisson's ratio
ρ	Mass density
σ_z	Stress amplitude
τ_{xz}	Shear stress amplitude
ω	Angular velocity